A nationwide regional flood frequency analysis at ungauged sites using ROI/GLS with copulas and super regions

Martin Durocher[1,*], Donald H. Burn[1] and Shabnam Mostofi Zadeh[1]

1 - Department of Civil and Environmental Engineering, University of Waterloo, 200 University Ave W, Waterloo (ON), Canada, N2L 3G1.

*Corresponding author: mduroche@uwaterloo.ca

Abstract

Region of influence is a common approach to estimate runoff information at ungauged locations. To estimate flood quantiles from annual maximum discharges, the Generalized Least Squares (GLS) framework has been recommended to account for unequal sampling variance and intersite correlation, which requires a proper evaluation of the sampling covariance structure. Since some jurisdictions do not have clear guidelines to perform this evaluation, a general procedure using copulas and a nonparametric intersite correlation model is investigated to estimate sampling covariance structure in situations where no common at-site distribution is imposed or when some paired sites do not have common periods of record. The investigated methodology is applied on 771 sites in Canada. The Normal copula is verified to be an adequate model that better fit paired observations than other types of extreme copulas. A sensitivity analysis is carried out to evaluate the impact of either ignoring, or considering a simpler form of, intersite correlation. Additionally, super regions are defined based on drainage area and mean annual precipitation to improve the calibration of pooling groups across large territories and a wide range of climate conditions. Performance criteria based on cross-validation revealed that using super regions and a combination of geographic distance and similarity between catchment descriptors improves the calibration of the pooling groups by providing more accurate estimates.

1. Introduction

26 To estimate flood quantiles at a site of interest where little or no streamflow information is available,

27 hydrologists and practitioners have relied on statistical models to predict runoff properties according to

28 available catchment descriptors. Countries such as the United States (IACWD, 1982), the United Kingdom

29 (Robson and Reed, 1999) and Australia (Ball et al. 2016) have adopted clear guidelines to standardize how

30 such analysis should be conducted. However, nationwide recommendations are not available in all

31 countries, including Canada. Recently, the project FloodNet (2015) was created as an initiative to

32 coordinate the efforts of experts in various fields, for improving the understanding of floods in Canada. In

33 this line, the present study investigates the problem of performing Regional Frequency Analysis (RFA) to

34 obtain flood quantiles at ungauged sites.

35 For Quebec and Ontario a previous study compared several combinations of delineation and prediction

36 methods (GREHYS, 1996a, 1996b). One general conclusion was that approaches based on the notion of

37 regions of influence (ROI), where each site is the center of its own pooling group, leads to better results

38 than the delineation of fixed regions. This finding is corroborated by other studies reported in Canada (Burn,

39 1990; Ribeiro-Corréa et al., 1995; Zrinji and Burn, 1994) and outside Canada (Eng et al., 2007; Merz and

40 Blöschl, 2005; Ouarda et al., 2008). Another conclusion was that the index-flood model (Dalrymple, 1960)

41 performed similarly to the direct estimation of the flood quantiles by regression (Thomas and Benson,

42 1975). Similar comparisons were repeated in a separate context with similar results (Durocher et al., 2016a;

43 Haddad and Rahman, 2012). Overall, the decision between these two approaches appears to be mostly

44 conceptual. One may argue that the index-flood model provides a more coherent framework by determining

45 the complete regional distribution, while the direct regression approach is more flexible and allows one to

46 easily mix sites with different types of distributions. The present study focuses on the direct regression

47 approach.

48 Flood frequency analysis is often performed over restricted geographic areas where boundaries are

49 determined by practical considerations. For instance, Canadian studies are generally performed at the

50 provincial level (El-Jabi et al., 2016; Gado and Nguyen, 2016; Sandrock et al., 1992), because water policies

51 fall within these jurisdictions. However, political boundaries are arbitrary from a hydrological perspective

52 and considering a larger database increases the amount of available information. On the other hand, a large

53 country such as Canada can have diverse climatic and flood regimes (Buttle et al., 2016). Therefore, a

54 nationwide analysis will also present additional challenges in the formation of the pooling groups and the

55 calibration of regression models. Many studies have reported a relation between the sample moments and

56 the drainage area or the mean annual precipitation (Basu and Srinivas, 2015; Blöschl and Sivapalan, 1997;

57 Meigh et al., 1997). In a study including sites in Italy, Austria and Slovakia, Salinas et al. (2014a) showed

58 that these two descriptors were proper surrogates for scale control and climate, which contribute to shape

59 the flood generating process. A classification of sites into super regions based on these surrogates could

60 provide a more meaningful solution for characterizing the outcomes of flood frequency analysis at a

61 national level than can be obtained using political regions.

62 An important decision when using ROI is the choice of a similarity measure that is necessary for creating

63 pooling groups centered around a target site. A distance between catchment descriptors is generally

64 preferred over geographical distance as the topography of nearby catchments can change quickly and lead

65 to distinct hydrological properties. Some studies have compared the usefulness of these two notions of

66 distance and showed that better predictions are generally obtained when considering both of them

67 simultaneously. In the United States, Eng et al.(2007) have successfully used a hierarchical approach where

68 the closest sites in terms of distance between descriptors are selected inside a bounded geographical area.

69 In contrast, Merz and Blöschl (2005) have found in an Austrian case study that superior predictive power

70   was found when using a spatial interpolation technique inside regions where a minimum of similarity

71   among the catchments was imposed. One possible explanation for these findings is that the set of available

72   catchment descriptors is not sufficient to fully characterize the flood generating process and hence,

73   geographical location represents a surrogate for missing descriptors that evolves smoothly in space. In

74   particular, for a study covering a large territory, such as Canada, the notion of geographical distance is

75   likely to be related to climate characteristics.

76   When using a regression model to estimate flood quantiles at ungauged sites the response variable is not

77   directly observed, but rather is estimated with different levels of uncertainty. Possible factors that contribute

78   in creating variations in the sampling variance include record lengths and observation scales (Tasker, 1980).

79   Additionally, large atmospheric systems that generate intense rainfall or build vast snowpacks can

80   simultaneously affect many sites. Omitting the impact of intersite correlation in RFA does not create bias

81   but does underestimate the model uncertainty (Bayazit and Önöz, 2004; Hosking and Wallis, 1988) and

82   reduces the power of homogeneity tests (Castellarin et al., 2008). Consequently, ignoring the spatial

83   component of the sampling can have important consequences on the decisions taken on the basis of a

84   selected model (Douglas et al., 2000; Madsen and Rosbjerg, 1997). Generalized Least Squares (GLS)

85   represents a natural approach to estimate parameters of a regression model that accounts for intersite

86   correlation and unequal variances. The model described in Tasker and Stedinger (1989) and considered in

87   several subsequent works (Haddad and Rahman, 2012; Kjeldsen and Jones, 2007; Madsen et al., 2002;

88   Robson and Reed, 1999), separates the total error into sampling and model components. In addition to a

89   better characterization of the source of variability, the approach was also shown to increase predictive

90   accuracies (Reis et al., 2005; Stedinger and Tasker, 1985; Vogel and Kroll, 1990).

91   Although GLS is considered as a good practice based on several studies, it has not been largely employed

92   in Canada. One reason to explain this low utilization may be the extra step required to evaluate the sampling

93   covariance structure. Across Canada, different regions of dominant nival, pluvial and mixed flood regimes

4

94　can be found (Burn et al., 2016). Therefore, it is reasonable to expect the existence of complex patterns of

95　spatial dependencies. However, Kroll and Stedinger (1998) indicated that using a smoothed version of the

96　intersite correlation structure has a relatively small impact on the predicted variability. Consequently,

97　several studies dealing with intersite correlations have preferred to accept some degree of approximation in

98　the sampling covariance matrix by using either Taylor approximation or by assuming simpler spatial

99　correlation models (Kjeldsen and Jones, 2004; Tasker and Stedinger, 1989). Moreover the evaluation of the

100　sampling may depend on the type of at-site distributions selected (Griffis and Stedinger, 2007), which

101　complicates the evaluation of the sampling covariance when no unique distribution is imposed.

102　The copula framework has gained popularity for describing non-traditional forms of spatial dependence

103　(Bárdossy, 2006; Gräler and Pebesma, 2011). Common assumptions in RFA are to consider the spatial

104　structure of a multivariate Normal distribution, which in terms of copula is equivalent to considering a

105　Normal copula (Durocher et al., 2016b; Renard, 2011). The Normal copula has also been considered in

106　RFA of extreme rainfall, but some studies have considered models based on the generalization of the

107　extreme value theory to spatial extremes, called max-stable processes, to provide more realistic

108　representation of the spatial dependence (Neves and Gomes, 2011; Shang et al., 2011; Westra and Sisson,

109　2011). In the copula framework, max-stable processes correspond to multivariate Husler-Reiss copula,

110　which has non-negligible probabilities that two extreme events occur jointly, which is not the case of the

111　Normal copula (Joe, 2015). Choosing a copula in RFA poses a similar dilemma to adopting, or not, the

112　GEV distribution in at-site frequency analysis as it is motivated by asymptotic arguments that assumes that

113　the maximums are taken over an infinite number of events. However, this assumption is not realistic in cold

114　regions, because the annual maximum discharge is generally the result of one event, the spring snowmelt.

115　The study of Wang et al. (2014) compared the performance of models based on max-stable processes and

116　regional L-moment algorithm (Hosking and Wallis, 1997) for extreme precipitation in Switzerland. When

117　correctly specified, the max-stable model improved the model fitting and the predicting capability, but when

118   misspecified it was shown to lead to non-negligible bias, which underlines the importance of correctly

119   choosing the copula when modeling spatial extremes.

120   The present study investigates the ROI/GLS framework when applied to a nationwide database that covers

121   vast territories and includes a large spectrum of climate conditions. Different models for estimating the

122   sampling covariance matrix are examined in light of the copula framework. Among them a nonparametric

123   model is proposed, which does not assume specific at-site distributions or estimation methods and remains

124   valid when few paired observations do not share common periods of record. In Canada, as far as the authors

125   know, there is no study that validates the choice of a proper copula for intersite correlation between floods.

126   One objective is to find such copula and to measure its impact on the estimation of flood quantiles. The

127   notion of super regions is also introduced in the context of ungauged analysis to help with calibrating and

128   understanding the outcomes of ROI/GLS regression models in terms of scale control and climate.

129   Additionally, the combination of geographical distance and distance between descriptors is explored to find

130   the right balance between them in the formation of pooling groups.

131   The present document is organized as follows. First, section 2 will describe the proposed ROI/GLS

132   methodology and its components. In section 3, the methods are applied on a large dataset of gauged sites

133   across Canada where different calibration of the regression models are examined in terms of quality of the

134   fitting and predictive performance. Finally, further discussions and conclusions are provided in section 4.

2. Methodology

136   The present methodology has three main components. First, an at-site frequency analysis of the gauged

137   sites is conducted to provide at-site estimates of flood quantiles. Second, an uncertainty analysis of the at-

138   site flood quantiles with return periods 10 and 100 years (denoted Q10 and Q100) is carried out including

139   the choice of a copula, the modeling of the intersite correlation and the estimation of a sampling covariance

140   matrix by Monte-Carlo simulation. Third, relationships between the flood quantiles and catchment

141 descriptors are characterized by the ROI/GLS approach and examined within super regions. The techniques

142 included in these three components are described in more detail below.

143 **2.1 At-site frequency analysis from annual maximums**

144 At-site frequency analysis based on annual maximums has a long tradition in hydrology and remains one

145 of the most common approaches for quantile estimation (Bezak et al., 2014). Theoretical arguments suggest

146 the utilization of Generalized Extreme Values (GEV) distribution, which arises as the limiting distribution

147 of blocks of maximums. However practical considerations often lead to the consideration of other types of

148 distributions. Identification of a best distribution remains an active debate (Salas et al., 2013). Guidelines

149 in the United States are to adopt the log-Pearson III (IACWD, 1982), while in the United Kingdom the

150 Generalized Logistic distribution is recommended (Robson and Reed, 1999). In Europe, Salinas et al.

151 (2014b) showed that even though the GEV often represents a good fit, it cannot accurately describe the

152 complete spectrum of hydrological diversities. Therefore, the present study will prioritize the GEV

153 distribution but will also consider alternative distributions when warranted; alternatives considered are the

154 Gumbel, Gamma, Pearson III, Normal, Generalized Normal and Generalized Logistic.

155 A classical approach for estimating the parameters of a statistical distribution is to maximize the data

156 likelihood (Coles, 2001). In the presence of a small sample size and heavy tails the maximum likelihood

157 estimator (ML) can sometimes have erratic behavior (Smith, 1985). Therefore, an estimator based on the

158 probability weighted moments, or equivalently the L-moments, is preferred (Hosking, 1990). In the present

159 study, the selection of the at-site distribution is established from a procedure that is guided by the Akaike

160 Information Criterion $AIC = 2k - 2l$, where k represents the number of parameters and l the log

161 likelihood (see, for instance, Di Baldassarre et al. (2009)). After identification of the best distribution in

162 terms of AIC, the AIC for the best distribution is compared to the AIC for the GEV distribution. If the

163 difference of AIC is less than one, the two distributions are assumed to fit the data equally well and the

164 GEV is selected. A comparison study of several statistical distributions was performed by Zhang et al.

165   (2018) and showed that the GEV is generally the best choice for Canadian Rivers. Therefore, the latter

166   criterion for judging the equivalence with the GEV is based on practical considerations and aims at selecting

167   alternative distributions only when this choice is not supported by the data. Note that a threshold of one in

168   this context is not very restrictive. In comparison, the addition of an extra parameter (for example passing

169   from Gumbel to GEV) increases the AIC by two and some authors even suggest a difference greater than

170   4 to be a meaningful difference (Burnham and Anderson, 2002).

171   The uncertainty analysis of the flood quantile estimates based on different types of at-site distributions is

172   not straightforward. In some analyses, the type of distribution is imposed, which allows the development

173   of simple approximate formulas (Bayazit and Önöz, 2004; Griffis and Stedinger, 2007; Kjeldsen and Jones,

174   2004). This is, however, not the case of the present study. Instead, Monte-Carlo simulations are considered

175   to approximate the sampling covariance matrix. The at-site frequency analysis is repeated 1000 times using

176   samples generated by parametric bootstraps. The covariance matrix is then computed empirically from

177   these samples. Although the method is computationally intensive, it is relatively simple to implement. The

178   simulations require the specification of a statistical model that accounts for the at-site distributions and the

179   intersite correlation.

180   **2.2 Intersite correlation in the copula framework**

181   A copula $C : [0,1]^d \rightarrow [0,1]$ is a multivariate distribution with uniform marginal distribution that respects

182   some basic properties (Nelsen, 2006). The fundamental advantage of the copula approach is the separation

183   of the dependence structure from marginal distributions. Commonly used multivariate distributions have

184   the following copula representation

185   (0) $$G(x_1, \ldots, x_d) = C\left[F_1\left(x_1\right), \ldots, F_d\left(x_d\right) \right],$$

186   where the F_i are the marginal distributions (Salvadori et al., 2007). For simulating a vector from G , one

187   can obtain first a uniform vector from copula C and then transform the output to the desired marginal

188   distribution using F_i^{-1}. This strategy is used to simulate one year of annual maximums where the marginal

189   distribution are the at-site distributions and the intersite correlation is described by a multivariate copula.

190   The Normal copula and t-copula characterize respectively the dependence of a multivariate Normal and

191   Student distribution. As in classical multivariate theory, the Normal copula is the limit case of a t-copula

192   when the degree of freedom is converging to infinity (Demarta and McNeil, 2005). Formally, the t-copula

193   is defined by

194   (0) $$C_{\Sigma,\upsilon}(u_1,\ldots,u_d) = t_{\upsilon,d}\left[t_{\upsilon,1}^{-1}(u_1),\ldots,t_{\upsilon,1}^{-1}(u_d);\Sigma\right],$$

195   where $t_{\upsilon,d}$ is the distribution function of a standard Student distribution of dimension d having degrees of

196   freedom υ and correlation matrix Σ . An important difference between the two copulas is a property called

197   upper tail dependence that is defined between two random variables $X_i \sim F_i$ with $i = 1,2$ as

198   (0) $$\lambda_{up} = \lim_{q \to 0^+} P\left[X_2 > F_2^{-1}(q) \mid X_1 > F_1^{-1}(q)\right].$$

199   For a t-copula, this property is controlled by the degrees of freedom where low values imply higher

200   probabilities that two extreme events occur jointly. At the opposite extreme, for the Normal copula $\lambda_{up} = 0$

201   , which means that two extreme values never occur together.

202   The validity of the choice of a copula C can be assessed by a goodness-of-fit test. For bivariate copulas,

203   extensive Monte-Carlo simulations showed that the test based on Cramer Von Mises statistics generally

204   leads to superior or competitive power in comparison to other alternatives (Berg, 2009; Genest et al., 2009).

205   However, such tests require many observations to discriminate between similar copulas. The idea of

206 assessing the quality of spatial models by examining paired observations inside a group of similar lag

207 distances using copula was first suggested by Bárdossy (2006). Although this approach does not provide a

208 formal test, rejection of the null hypothesis for some lag distance provides evidence of model

209 misspecification. That strategy was later formalized by Durocher and Quessy (2017), who showed from

210 simulation studies that reasonable power can be expected in realistic settings.

211 For t-copulas, the coefficients of correlation for Σ can be estimated by a moment-based estimator and once

212 known, the degrees of freedom are estimated by maximum likelihood (Lindskog et al., 2003). Spearman

213 rank correlation coefficient, or simply Spearman's rho ρ is defined as the correlation between the ranks of

214 two variables. For the t-copula, there is a one-to-one relation between the Spearman's rho and one

215 coefficient θ of Σ:

216 (0) $$\theta = 2\sin\left(\frac{\pi}{6}\rho\right).$$

217 In an ideal situation, all pairs of sites will have enough years of common record to ensure a reliable estimate

218 of ρ and Σ. However, for different practical reasons, paired observations are recorded over different

219 periods of time and so may prevent or lead to unreliable estimates of ρ . In that case, a spatial correlation

220 model is necessary to have estimates at every pair of sites (Schabenberger and Gotway, 2004). A common

221 choice of spatial correlation model is the power exponential model (POW) where the correlation function

222 s in respect of distance h is

223 (0) $$s(h) = \begin{cases} (1-\tau)\exp\left[-3\left(\dfrac{h}{\alpha}\right)^{\gamma}\right] & h \neq 0 \\ \\ 1 & h = 0 \end{cases}$$

224   where $\alpha > 0$ controls the strength of the correlation, $0 \le \tau \le 1$ is a nugget effect and $0 < \gamma \le 2$ is a

225   smoothing parameter. This correlation model is attractive for its simplicity, but may not adequately fit all

226   complex situations. For this reason, a nonparametric model that is more flexible is also considered. Let h_{ij}

227   be the distance (km) between a pair of sites i and j and define the average drainage area A_{ij} (km^2),

228   longitude x_{ij} and latitude y_{ij} for the pair (i, j). The nonparametric model characterizing the intersite

229   correlation is

230   (0) $\qquad\qquad g(\rho_{ij}) = f_h(h_{ij}) + f_A(A_{ij}) + f_{xy}(x_{ij}, y_{ij}) + e_{ij}$

231   where g is the Fisher z-transformation

232   (0) $\qquad\qquad g(\rho_{ij}) = \dfrac{1}{2} \log\left(\dfrac{1 + \rho_{ij}}{1 - \rho_{ij}} \right) ;$

233   f_h, f_A and f_{xy} are smooth continuous functions and e_{ij} is an error term. A model of this form falls under the

234   umbrella of generalized additive model where an in-depth description is provided for instance in Wood

235   (2006). The Fisher transformation is used to transform the empirical Spearman's rho ρ_{ij} between -1 and 1

236   to a near normal distribution. The smooth functions f_h, f_A and f_{xy} are thin plate regression splines, which

237   are well suited for modeling spatial covariates (Wood, 2003). To avoid overfitting the estimation process

238   is regularized by penalized least squares (Green and Silverman, 1993). The evolution of the Spearman's rho

239   in respect of the distance is described by f_h, which plays a similar role to the POW model. The other

240   components, f_A and f_{xy}, characterize other components of the intersite correlation. In particular,

241     $f_{xy}(x_{ij}, y_{ij})$ adjusts the intersite correlation on the basis of the paired locations.

242 Estimation of Σ is deduced using equation (0) and fitted ρ_{ij}. However, the matrix Σ derived directly from

243 the nonparametric model will not in general be positive definite, which leads to numerical problems and so

244 the algorithm of Higham (2002) is used to find the nearest matrix that respects this condition.

2.3 Regression models using GLS

246 Flood quantiles are modeled by a multiple regression model at the logarithm scale for sites found inside a

247 pooling group with regression equation

248 (0) $\qquad \mathbf{y} = \mathbf{X}\boldsymbol{\beta} + \boldsymbol{\omega}$

249 where $\mathbf{X} \in \mathbb{R}^p$ is a design matrix of relevant catchment descriptors and $\boldsymbol{\omega}$ is an error term. Due to the

250 uncertainty resulting from at-site estimation, it is assumed that the response variable $\mathbf{y} = (y_1, \ldots, y_n)$ has

251 a sampling error $\boldsymbol{\epsilon} = \epsilon_1, \ldots, \epsilon_n$, with covariance matrix $E(\boldsymbol{\varepsilon\varepsilon}') = \Sigma$ as described above. Stedinger and

252 Tasker (1985) proposed considering a second term of error $\boldsymbol{\eta}$ of variance $\sigma_\eta^2 > 0$ that is independent and

253 identically distributed. Overall, the total error $\boldsymbol{\omega} = \boldsymbol{\eta} + \boldsymbol{\epsilon}$ has covariance matrix

254 (0) $\qquad \Lambda\left(\sigma_\eta^2\right) = \sigma_\eta^2 I + \Sigma$,

255 which provides a better characterization of the multiple sources of variability. Notice that the total

256 covariance matrix is dependent on an unknown parameter σ_η^2 that describes the model variance, *i.e.* the

257 part of the total variance that is not due to sampling.

258 For a known model variance σ_η^2, the total covariance matrix can be rewritten $\Lambda\left(\sigma_\eta^2\right) = \sigma_\eta^2 \mathbf{G}$. Computing

259 $\mathbf{G} = \mathbf{U}^T \mathbf{U}$ by Cholesky decomposition allows reformulating the GLS problem as an ordinary least squares

260   (OLS) problem with transformed response variable $\mathbf{y}^{*} = \mathbf{U}^{-T}\mathbf{y}$ and design matrix $\mathbf{X}^{*} = \mathbf{U}^{-T}\mathbf{X}$. Therefore,

261   the GLS estimator and its covariance matrix are derived directly from classical OLS theory:

262   (0) $$\hat{\boldsymbol{\beta}} = \left[\mathbf{X}'\mathbf{G}^{-1}\mathbf{X} \right]^{-1} \mathbf{X}\mathbf{G}^{-1}\mathbf{y}$$

263   (0) $$\Sigma_{\hat{\boldsymbol{\beta}}} = \sigma_{\boldsymbol{\eta}}^{2} \left[\mathbf{X}^{T}\mathbf{G}^{-1}\mathbf{X} \right]^{-1} \quad .$$

264   Moreover, the residuals can be linked to the GLS residuals

265   (0) $$\tilde{\omega} = \mathbf{y}^{*} - \mathbf{X}^{*}\hat{\boldsymbol{\beta}} = \mathbf{U}^{-T}\omega \ ,$$

266   which has residual variance corresponding to the model variance $\sigma_{\boldsymbol{\eta}}^{2}$. In general, the model variance $\sigma_{\boldsymbol{\eta}}^{2}$

267   is unknown and a proper estimation can be obtained by iterative least squares (Kjeldsen and Jones, 2009).

268   The procedure consists in estimating the model parameters $\boldsymbol{\beta}$ from an initial guess obtained by OLS and

269   to update $\sigma_{\boldsymbol{\eta}}^{2}$ using the empirical variance of GLS residuals in equation (0). These two steps are repeated

270   until convergence.

271   **2.4 Pooling groups and super regions**

272   Pooling groups are formed of the M sites that are the closest to the target site. To that end, three types of

273   distance are considered: The geographical distance (GEO), the Mahalanobis distance between catchment

274   descriptors (PHY) and the canonical distance. The Mahalanobis distance is selected because it considers

275   not only the scales of the catchment descriptors, but also their covariance structure, which accounts for

276   information redundancy (Cunderlik and Burn, 2006). The study of Oudin et al. (2010) showed that regions

277   based on the similarity among catchment descriptors do not always easily translate into similarity in terms

278   of hydrological properties. Consequently, regions derived from these two notions may lead to very different

279 groups of sites. Canonical correlation analysis (CCA) can be used to create new canonical coordinates in

280 the hydrological space that are mutually independent and sequentially maximizes correlation with

281 catchment descriptors. The canonical distance defined as the distance between the canonical coordinates

282 was used in RFA to delineate homogenous regions (Ouarda et al., 2001; Spence et al., 2007) or to perform

283 spatial interpolation of the outcomes of hydrological models (Hundecha et al., 2008). For ungauged

284 analysis, the hydrological information is unknown, but a substitute target position is estimated using the

285 correlation with the catchment descriptors. Therefore the quality of the canonical distance for pooling

286 groups depends on the relevance of the canonical distance and the quality of the estimated target in the

287 canonical space (Durocher et al., 2016a).

288 The present study considers the formation of pooling groups directly using one of the three distances

289 mentioned, but also considering combinations of two distance measures using a hierarchical approach.

290 Specifically, the procedure involves identifying for each site a subset of M_1 sites located the closest to the

291 target based on the first distance and then forming a pooling group of size $M_2 \leq M_1$ based on the second

292 distance measure. For instance, a subset of the 100 nearest sites is extracted using the GEO distance and

293 then a pooling group of size 25 sites is selected among them based on the PHY distance. Such approach

294 will be denoted as GEO-PHY distance. This strategy is similar to the approach of Eng et al. (2007) that

295 used pooling groups based on the PHY distance, but where a fixed distance was used instead of a constant

296 number of sites.

297 If a pooling group contains too few sites, it will lead to a large predictive variance, but including many sites

298 that are not relevant to the site of interest may create bias. In addition to the size of the pooling group, the

299 choice of the catchment descriptors can also influence the quality of the fitting. To guide the calibration of

300 a pooling group, it is recommended to find settings that optimize the quality of the prediction (Reis et al.,

301 2005). Let y_0 be the flood quantiles at an ungauged location that has catchment descriptors $\mathbf{x}_0$. Using the

302 GLS estimator in equation (0) the predictive variance is given by

14

303 (0) $$\sigma_{\eta}^2\left[1+\mathbf{x}_0^T\left(\mathbf{X}^T\mathbf{G}^{-1}\mathbf{X}\right)^{-1}\mathbf{x}_0\right],$$

304 which can be optimized by comparing various combinations of pooling group size and catchment

305 descriptors.

306 Another strategy for the calibration of the ROI/GLS model consists in selecting the same size and catchment

307 descriptors for a group G of sites. Notice that these groups will only be used for calibration and do not

308 affect the formation of the pooling groups. Although such groups could take different forms, the present

309 study defines super regions according to site drainage area and mean annual precipitation. Similar super

310 regions were considered by Salinas et al. (2014a), but instead of using 3 straightforward divisions (i.e.,

311 small, medium and large), the present study uses a hierarchical agglomerative clustering method (Murtagh

312 and Legendre, 2014; Ward, 1963) to provide more objective boundaries, while maintaining meaningful

313 interpretation.

314 Inside a super region, the prediction performance associated with specific settings can be evaluated by

315 cross-validation. Formally, let $y_{(i)}$ be predicted flood quantiles (log) obtained at the i-th site when it is

316 considered ungauged. Optimal settings may be identified by minimizing a criterion based on the predicted

317 residuals $y_i - y_{(i)}$. In this line, two common performance criteria are the Nash-Sutcliffe and the mean

318 absolute deviation

319 (0) $$\mathrm{NSH} = 100 \times \left\{ 1 - \frac{\sum\limits_{i \in G} w_i \left(y_i - y_{(i)}\right)^2}{\sum\limits_{i \in G} w_i \left(y_i - \bar{y}\right)^2} \right\} \quad \text{and} \quad \mathrm{MAD} = \frac{\sum\limits_{i \in G} w_i \left|y_i - y_{(i)}\right|}{\sum\limits_{i \in G} w_i},$$

320 where w_i are weights such that $\sum_i w_i = 1$ and $\bar{y}$ is the weighted average of the y_i. For the calibration of

321 the ROI/GLS model, the weights are taken as the record length of a site, which gives more importance to

322 sites with more data.

3.Results

3.1 Data

The annual maximums of river discharge are extracted from daily records provided by Water Survey of Canada (2017) and catchment descriptors are provided by Environment and Climate Change Canada. Figure 1 presents the locations of 771 selected sites where the desired catchment descriptors were available. Every site is verified to possess at least 20 years of records and not exhibit significant trends according to the Mann Kendall test (Önöz and Bayazit, 2012).

The concept of super regions is to improve the interpretability of the results by dividing sites with similar scale control and climate. After some experimentation, the sites were divided into 8 super regions. Figure 2 presents the correspondence between position in the descriptor space and their locations. Super region 1 uniquely includes sites from the Pacific coast having small to medium drainage area and the largest mean annual precipitation. Other wetter sites are found in super regions 2 to 4, which are located either in British Columbia or in the southeastern part of Canada. The drier ones correspond to super regions 5 to 8, which are mostly located in the prairie provinces (Alberta, Saskatchewan and Manitoba) and in the northern part of Canada. In general, the largest watersheds are found in the more northerly locations and correspond to super regions 7 and 8. In particular, super region 7 is wetter than super region 8 and is located mostly in the north of Quebec, Ontario and British Columbia. One can see that British Columbia includes a large variety of rivers as it includes sites from the eight super regions. Table 1 presents descriptive statistics for the drainage area and mean annual precipitation as well as the other available catchment descriptors, which include: basin compactness, average slope, streamflow density, percentage of waterbody area and site elevation.

The fitting and the selection of the best distribution at each gauged site is performed as described in the methodology section. The GEV distribution (including Gumbel) was preferred in 62.5 % of the gauged

16

346   sites, followed by the Pearson type III (including Gamma) with 29.7 %. The other distributions were

347   selected in lower proportions. The flood quantiles associated with return levels are then computed for each

348   site using the selected distribution.

349   **3.2 Estimation of the sample covariance matrix**

350   The correlation matrix of Spearman's rho coefficient is estimated using the nonparametric model in equation

351   (0), where an adjusted coefficient of determination (R^2) of 52% is obtained, indicating that the model fits

352   the data fairly well. The relative importance of each smooth term is assessed by examining the difference

353   of R^2 when that component is removed. As expected, the most important smooth term is f_h associated with

354   the distance and has a relative importance of 21%. It is followed respectively by f_{xy} and f_A with 13%

355   and 2 %. These values indicate that the intersite correlation is mostly influenced by the distance between

356   sites, but that a non-negligible effect is also depending mostly on the location. In other words, the

357   dependence among pairs of sites cannot be explained uniquely by the separating distance. The effect of f_{xy}

358   is illustrated in Figure 3 using a map of the smoothed terms, even though discharge can only be observed

359   at unique points on rivers. One can see different zones where the Spearman's rho is lower or higher than

360   what would be expected considering uniquely f_h, the effect of the distance between sites.

361   Figure 3 also shows the correlation coefficient in respect of the distance where the solid line represents the

362   POW model fitted by weighted least squares using record lengths as weights; with parameters $\alpha = 905$, τ

363   = 0.14 and γ = 0.81. Notice that the coefficient of correlation in respect of the distance becomes (in

364   average) stable after roughly 600 km, but never reaches zero. The POW model is biased after that point as

365   it can be assumed that for separations beyond 600 km, the correlation becomes more and more negligible.

366   From a practical point of view, after 600 km the correlation is relatively low (less than 0.2). It is then

367   reasonable to assume that it decreases to values that are not statistically different from zero.

368 The choice of a copula is investigated to determine the nature of the dependence among near sites. As the

369 power for rejecting the null hypothesis increases with the strength of the dependence, only paired

370 observations separated by less than 50 km and having at least 40 years of common record are selected. In

371 total, 109 paired observations are identified and are presented in Figure 1. Note that the minimum

372 Spearman's rho for these paired observations is 0.7. For each pair, goodness-of-fit tests are performed using

373 as null hypothesis one of the following copulas: Normal, t-copula, Husler-Reiss, Gumbel, Galambos and

374 Clayton (see, for instance, Salvadori et al. (2007) for a description of these copulas). The results show that

375 only the Clayton copula is rejected at a significance level 5% in a majority of the cases, while the other

376 copulas are not rejected for all pairs. In the present study, the size of the sample remains relatively small

377 and so the goodness-of-fit tests do not have high power of discrimination. Nevertheless, these results do

378 not indicate any evidence that would suggest rejecting these copulas.

379 Figure 4 presents a comparison of the log-likelihood between the bivariate Normal copula in respect of two

380 bivariate extreme copulas. One can see that for most paired observations, the Normal copula provides the

381 best fit as evidenced by there being more points below than above the 45° line. In particular, it suggests a

382 preference for a multivariate Normal copula over a max-stable process to characterize the spatial

383 dependence among all observations. The decision between the Normal copula or t-copula will affect the

384 behavior in terms of tail dependence. Fitting a multivariate t-copula on all paired observations led to

385 estimated degrees of freedom $\upsilon = 15$, which is associated with a relatively low tail dependence. For

386 instance, with correlation coefficient of 0.5 and 0.3 the tail dependence is respectively 0.03 and 0.01. This

387 agrees with the better fit of the bivariate Normal copula in comparison to extreme copulas for which tail

388 dependence is an important characteristic. Therefore, the Normal copula is adopted as a reasonable model

389 for the rest of the analysis.

390 The matrix of sampling covariances for the flood quantiles (log) is obtained for several return periods using

391 Monte-Carlo simulations as described in the methodology. Figure 5 (left panel) illustrates the correlation

392   between the paired Q100 in respect of the distance and the solid line represents the fitted POW model.

393   Similarly, the right part of Figure 5 shows fitted POW model for various return periods. One can see that

394   the strength of the correlation decreases with the return period. On average, the correlation between Q100

395   becomes less than 0.2 after roughly 100 km, while intersite correlation between annual maximum reach

396   that point more around 400 km. Note that the zero tail dependence property of the Normal copula implies

397   that for very large return periods the correlation between flood quantiles will continue to decrease towards

398   zero.

399   **3.3 Calibration of the pooling groups**

400   As described in the methodology, the calibration of the ROI/GLS models may be guided by the predictive

401   variance, equation (0), or by cross-validation, equation (0). In the following, each site is treated in turn as

402   ungauged and a regression model is fitted using several combinations of pooling group sizes and catchment

403   descriptors. More precisely, the pooling group sizes $M_2 = 20, 25, \ldots, 80$ and all combinations of three or

404   more catchment descriptors are tried. The initial subset inside which the pooling groups are formed is

405   restricted to $M_1 = 100$ or 200.

406   Table 2 presents the prediction performance obtained using different distances and comparing the

407   calibration obtained using the predictive variance (Individual) and the criterion MAD inside super regions.

408   Note that only the best hierarchical distances are reported. For GEO-PHY and GEO-CCA this corresponds

409   to $M_1 = 100$ sites, while for PHY-GEO, $M_1 = 200$ sites. When the predictive variance is used, the

410   geographical distance led to better predictive performance than the other distance in terms of MAD for both

411   Q10 and Q100. However, all the results are relatively similar in terms of NSH, except for the direct

412   canonical distance that has poorer performance. Nevertheless, better predictive performances are always

413   found when the models are calibrated using super regions. In these cases, the GEO-PHY and the PHY-GEO

414   distance perform similarly with a slight advantage to GEO-PHY. This illustrates the clear advantage of

415 combining these two distances. In particular, the hierarchical approach GEO-CCA performs substantially

416 better than the direct use of the canonical distance.

417 One objective of the present study is to examine the advantage of a nationwide analysis in comparison to

418 an analysis based on smaller geographical areas. To explore this impact, the calibration of the ROI/GLS

419 model is split in four distinct administrative regions. The first region regroups the four Atlantic provinces

420 (New Brunswick, Nova Scotia, Prince Edward Island and Newfoundland and Labrador) with 90 sites. The

421 second region combines Ontario and Quebec with 180 sites, while the third region regroups British

422 Columbia and Yukon Territory with 213 sites. The Prairies and the two remaining territories complete the

423 fourth region with 288 sites. For each region, 3 super regions were delineated inside. Note that these settings

424 do not represent all possibilities that involve administrative boundaries. Nevertheless, it should illustrate

425 the potential impact this has on the calibration of ROI/GLS. When using a nationwide analysis, the

426 performance criteria for Q100 using the GEO-PHY distance are NSH = 91.05 and MAD = 0.343. The same

427 criteria are slightly inferior when using administrative boundaries with NSH = 90.77 and MAD = 0.351.

428 Similar outcomes are observed with Q10 where performance criteria pass from NSH = 93.49 and MAD =

429 0.296 to NSH = 92.85 and MAD = 0.317, respectively.

430 The results obtained in the present study are coherent with previous studies for portions of Canada. In the

431 province of Quebec (Durocher et al., 2016a) and Ontario (Grover et al., 2002) relative root mean square

432 errors (RRMSE) of 0.435 and 0.347 were reported for Q100. When using similar metrics, the ROI/GLS

433 method used in the present study finds RRMSE of 0.438 and 0.346. However, such comparison must be

434 done with care as these studies don't consider exactly the same set of gauged sites and were conducted on

435 different periods.

3.4 Uncertainty analysis

436

437 Overall the best ROI/GLS models are obtained using super regions and the GEO-PHY distance, which is

438 now examined in more detail. Table 3 reports the sizes and catchment descriptors used in the pooling groups

439 of each super region and Table 4 separates the predictive performance by super regions. The wetter super

440 region 1 and the larger super region 8 are well fitted with NSH greater than 90 for both flood quantiles;

441 these super regions also have the lowest MAD. Good predictive performance is also observed for the wetter

442 super regions 2 to 4. The prediction of the drier sites mostly found in the Prairies and the north is, however,

443 relatively less accurate, especially for the smaller watersheds in super regions 5 and 6, with respective NSH

444 of 32.23 and 65.43. These lower predictive performances are largely due to the presence of problematic

445 sites. Figure 6 presents the predicted residuals standardized by the predictive variance. For Q10, one

446 potential outlier is found in super region 5 where the predictive residual is higher than 8 standard deviations.

447 For Q100, the same site remains problematic and other potential outliers arise in super region 6. This finding

448 suggests that smaller and drier sites are more likely to be problematic to estimate than those of the other

449 super regions. When predictive residuals higher than 3 standard deviations are removed for Q100, the NSH

450 of super regions 5 and 6 is much better and becomes 76.02 and 73.35, respectively. Note that the NSH

451 criterion evaluates the predictive performance in comparison to the weighted average, but does not represent

452 a measure of the absolute uncertainty. For instance, super region 3 includes medium sized catchments

453 strongly concentrated in southern Ontario. The NSH of Q100 for this super region is 69.72 which is less

454 than super region 7 with 84.85. However, the MAD of super region 3 is 0.29 in comparison to 0.38 for

455 super region 7, showing that estimations are overall less uncertain. Even after removing outliers, the

456 estimation of the flood quantiles Q10 and Q100 for the drier super regions 5 to 7 remain less accurate with

457 MAD greater than 0.33, while less than 0.29 for the other super regions.

458 A sensitivity analysis is conducted to measure the effect of the intersite correlation model used to obtain

459 the sampling covariance matrix on variability of the estimated flood quantile. Let σ_{IND}^2, σ_{POW}^2 and σ_{NP}^2

460 denote the predictive variance obtained assuming intersite independence, the POW model and the

461 nonparametric model. The nonparametric model is more flexible and so its predictive variance should be

462 closer to the true value. Consequently σ_{NP}^2 is considered as a benchmark and Figure 7 shows the ratio of

463 variance $\sigma_{POW}^2 / \sigma_{NP}^2$ (left) and $\sigma_{IND}^2 / \sigma_{NP}^2$ (right). The ROI/GLS model was calibrated using the GEO

464 distance (top) and the GEO-PHY distance (bottom). The ratios $\sigma_{POW}^2 / \sigma_{NP}^2$ of both distances (left) show

465 that a smoother version of the intersite correlation has a limited impact on the evaluation of the model

466 uncertainties, while the assumption of independence tends to underestimate it. In particular, the

467 underestimation of the model uncertainties is affecting more the drier and larger basins found in super

468 regions 3, 6, 7 and 8. Figure 7 (bottom-right) indicates that even though the distance GEO-PHY mainly

469 formed the pooling group based on the distance between catchment descriptors, there is a substantial impact

470 on the estimation of predictive variance from the covariance model. However, this underestimation is as

471 expected less important than when using the GEO distance (top-right) that forces stronger intersite

472 correlations in the pooling groups.

4. Conclusions

474 The ROI/GLS method was investigated to estimate flood quantiles at ungauged locations using a large

475 database of 771 sites across Canada. The calibration procedure provides a general guideline to apply

476 ROI/GLS regression in situations where no direct formula is available for evaluating the sample covariance

477 matrix. A pairwise fitting of copulas was considered among close sites to show that the Normal copula is a

478 reasonable model for the intersite correlation structure. In particular, it reveals that extreme type of spatial

479 dependence is not generally the best option for characterizing the relationship among annual maximum

480 streamflow in Canada. Similar findings should be expected in other cold regions, because floods are

481 dominated by spring snowmelt. Such behavior goes in the opposite direction to the recent interest in the

482 max-stable processes in the characterization of spatial dependence between extreme rainfall events.

483   A nonparametric model was used to estimate the sampling covariance matrix of various pairs of flood

484   quantiles. This approach was selected to better estimate the associations between paired observations when

485   there are few or no years of common record. The main objective of using GLS in RFA is to obtain accurate

486   estimation of the uncertainties of flood quantiles. In this regard, it was found that a simpler intersite

487   correlation structure characterized by a power exponential model in respect of the geographical distance

488   does not largely affect the estimation of the predictive variance and led to similar evaluation of the

489   predictive variance. However, ignoring intersite correlation was shown to underestimate the predictive

490   variance substantially. This is especially true for the drier basins located mostly in the Prairies and in the

491   northern part of the country.

492   Cross-validation was used to evaluate and guide the calibration of the ROI/GLS models using three notions

493   of distance. It was shown that the best choice was a hierarchical approach where first the 100 nearest sites

494   to the target are identified according to the geographical distance and then a smaller pooling group is formed

495   using the Mahalanobis distance between catchment descriptors. Additionally, super regions were delineated

496   based on the drainage area and the mean annual precipitation to help the calibration of the ROI/GLS model.

497   For each super region the same catchment descriptors and pooling group sizes were chosen. This strategy

498   led to better predictive power than individually calibrating sites using the predictive variance. The effect of

499   administrative boundaries on the calibration of the regression models was also explored. The results showed

500   that performing a nationwide RFA analysis resulted in ROI/GLS models with better predictive power. The

501   concept of super regions was also found useful to calibrate the pooling groups and to better understand the

502   quality of the flood estimations in respect of scale control and climate. The results indicated that the flood

503   quantiles of the drier basins are estimated with greater uncertainty than the wetter ones. In particular,

504   ROI/GLS resulted in rather poor predictions for some problematic sites in some of the smaller and drier

505   basins.

506 Overall, the present study validates successful settings to carry out RFA using the ROI/GLS framework. In

507 particular, it provides guidelines for estimating the sampling covariance matrix in a general context and

508 using super regions to improve the calibration of the pooling groups. These outcomes are helpful to promote

509 the adoption of GLS in RFA.

510 Acknowledgements

514

References

Ball, J.E., Babister, M.K., Nathan, R., Weinmann, P.E., Weeks, W., Retallick, M., Testoni, I., 2016. Australian Rainfall and Runoff - A Guide to Flood Estimation. Commonwealth of Australia.

Basu, B., Srinivas, V.V., 2015. A recursive multi-scaling approach to regional flood frequency analysis. Journal of Hydrology 529, 373–383. https://doi.org/10.1016/j.jhydrol.2015.07.037

Bárdossy, A., 2006. Copula-based geostatistical models for groundwater quality parameters. Water Resources Research 42. https://doi.org/10.1029/2005WR004754

Bayazit, M., Önöz, B., 2004. Sampling variances of regional flood quantiles affected by intersite correlation. Journal of Hydrology 291, 42–51. https://doi.org/10.1016/j.jhydrol.2003.12.009

Berg, D., 2009. Copula goodness-of-fit testing: an overview and power comparison. The European Journal of Finance 15, 675–701. https://doi.org/10.1080/13518470802697428

Bezak, N., Brilly, M., Šraj, M., 2014. Comparison between the peaks-over-threshold method and the annual maximum method for flood frequency analysis. Hydrological Sciences Journal 59, 959–977. https://doi.org/10.1080/02626667.2013.831174

Blöschl, G., Sivapalan, M., 1997. Process controls on regional flood frequency: Coefficient of variation and basin scale. Water Resour. Res. 33, 2967–2980. https://doi.org/10.1029/97WR00568

Burn, D.H., 1990. An appraisal of the "region of influence" approach to flood frequency analysis. Hydrological Sciences Journal 35, 149–165. https://doi.org/10.1080/02626669009492415

Burn, D.H., Whitfield, P.H., Sharif, M., 2016. Identification of changes in floods and flood regimes in Canada using a peaks over threshold approach. Hydrol. Process. 30, 3303–3314. https://doi.org/10.1002/hyp.10861

Burnham, K.P., Anderson, D.R., 2002. Model Selection and Multimodel Inference: A Practical Information-Theoretic Approach, Springer Science & Business Media.

Buttle, J.M., Allen, D.M., Caissie, D., Davison, B., Hayashi, M., Peters, D.L., Pomeroy, J.W., Simonovic, S., St-Hilaire, A., Whitfield, P.H., 2016. Flood processes in Canada: Regional and special aspects. Canadian Water Resources Journal / Revue canadienne des ressources hydriques 41, 7–30. https://doi.org/10.1080/07011784.2015.1131629

Castellarin, A., Burn, D.H., Brath, A., 2008. Homogeneity testing: How homogeneous do heterogeneous cross-correlated regions seem? Journal of Hydrology 360, 67–76. https://doi.org/10.1016/j.jhydrol.2008.07.014

Coles, S., 2001. An introduction to statistical modeling of extreme values. Springer Verlag.

Cunderlik, J.M., Burn, D.H., 2006. Switching the pooling similarity distances: Mahalanobis for Euclidean. Water Resour. Res. 42, W03409. https://doi.org/10.1029/2005WR004245

Dalrymple, T., 1960. Flood-frequency analysis. Survey Water-Supply Paper 1543.

Demarta, S., McNeil, A.J., 2005. The t Copula and Related Copulas. International Statistical Review 73, 111–129. https://doi.org/10.1111/j.1751-5823.2005.tb00254.x

Di Baldassarre, G., Laio, F., Montanari, A., 2009. Design flood estimation using model selection criteria. Physics and Chemistry of the Earth, Parts A/B/C, Recent developments of statistical tools for hydrological application 34, 606–611. https://doi.org/10.1016/j.pce.2008.10.066

554   Douglas, E.M., Vogel, R.M., Kroll, C.N., 2000. Trends in floods and low flows in the United States:
555   impact of spatial correlation. Journal of Hydrology 240, 90–105. https://doi.org/10.1016/S0022-
556   1694(00)00336-X

557   Durocher, M., Chebana, F., Ouarda, T.B.M.J., 2016a. Delineation of homogenous regions using
558   hydrological variables predicted by projection pursuit regression. Hydrol. Earth Syst. Sci. 20,
559   4717–4729. https://doi.org/10.5194/hess-20-4717-2016

560   Durocher, M., Chebana, F., Ouarda, T.B.M.J., 2016b. On the prediction of extreme flood quantiles at
561   ungauged locations with spatial copula. Journal of Hydrology 533, 523–532.
562   https://doi.org/10.1016/j.jhydrol.2015.12.029

563   Durocher, M., Quessy, J.-F., 2017. Goodness-of-fit tests for copula-based spatial models. Environmetrics
564   n/a-n/a. https://doi.org/10.1002/env.2445

565   El-Jabi, N., Caissie, D., Turkkan, N., 2016. Flood analysis and flood projections under climate change in
566   New Brunswick. Canadian Water Resources Journal 41, 319–330.
567   https://doi.org/10.1080/07011784.2015.1071205

568   Eng, P. C. Milly, Gary D. Tasker, 2007. Flood Regionalization: A Hybrid Geographic and Predictor-
569   Variable Region-of-Influence Regression Method. Journal of Hydrologic Engineering 12, 585–
570   591. https://doi.org/10.1061/(ASCE)1084-0699(2007)12:6(585)

571   Floodnet, 2015. Floodnet - NSERC Network - Enhanced flood forecasting and management capacity in
572   Canada [WWW Document]. URL http://www.nsercfloodnet.ca/ (accessed 7.26.17).

573   Gado, T.A., Nguyen, V.-T.-V., 2016. Comparison of Homogenous Region Delineation Approaches for
574   Regional Flood Frequency Analysis at Ungauged Sites. https://doi.org/10.1061/(ASCE)HE.1943-
575   5584.0001312

576   Genest, C., Rémillard, B., Beaudoin, D., 2009. Goodness-of-fit tests for copulas: A review and a power
577   study. Insurance: Mathematics and economics 44, 199–213.
578   https://doi.org/10.1016/j.insmatheco.2007.10.005

579   Gräler, B., Pebesma, E., 2011. The pair-copula construction for spatial data: a new approach to model
580   spatial dependency. Procedia Environmental Sciences 7, 206–211.
581   https://doi.org/10.1016/j.proenv.2011.07.036

582   Green, P.J., Silverman, B.W., 1993. Nonparametric regression and generalized linear models: a roughness
583   penalty approach. Chapman & Hall/CRC.

584   GREHYS, 1996a. Presentation and review of some methods for regional flood frequency analysis.
585   Journal of Hydrology 186, 63–84.

586   GREHYS, 1996b. Inter-comparison of regional flood frequency procedures for canadian rivers. Journal of
587   hydrology(Amsterdam) 186, 85–103.

588   Griffis, V.W., Stedinger, J.R., 2007. The use of GLS regression in regional hydrologic analyses. Journal
589   of Hydrology 344, 82–95. https://doi.org/10.1016/j.jhydrol.2007.06.023

590   Grover, P.L., Burn, D.H., Cunderlik, J.M., 2002. A comparison of index flood estimation procedures for
591   ungauged catchments. Can. J. Civ. Eng. 29, 734–741. https://doi.org/10.1139/l02-065

592   Haddad, K., Rahman, A., 2012. Regional flood frequency analysis in eastern Australia: Bayesian GLS
593   regression-based methods within fixed region and ROI framework – Quantile Regression vs.
594   Parameter Regression Technique. Journal of Hydrology 430–431, 142–161.
595   https://doi.org/10.1016/j.jhydrol.2012.02.012

596   Higham, N.J., 2002. Computing the nearest correlation matrix—a problem from finance. IMA J Numer
597   Anal 22, 329–343. https://doi.org/10.1093/imanum/22.3.329

598   Hosking, J.R.M., 1990. L-Moments: Analysis and Estimation of Distributions Using Linear Combinations
599   of Order Statistics. Journal of the Royal Statistical Society. Series B (Methodological) 52, 105–
600   124.

601   Hosking, J.R.M., Wallis, J.R., 1997. Regional frequency analysis: an approach based on L-moments.
602   Cambridge Univ Pr.

603   Hosking, J.R.M., Wallis, J.R., 1988. The effect of intersite dependence on regional flood frequency
604   analysis. Water Resour. Res. 24, 588–600. https://doi.org/10.1029/WR024i004p00588

605   Hundecha, Y., Ouarda, T.B.M.J., Bárdossy, A., 2008. Regional estimation of parameters of a rainfall-
606   runoff model at ungauged watersheds using the "spatial" structures of the parameters within a
607   canonical physiographic-climatic space. Water Resources Research 44.
608   https://doi.org/10.1029/2006WR005439

609   Interagency Committee on Water Data (IACWD), 1982. Guidelines for determining flood flow
610   frequency : Bulletin 17-B (revised and corrected). Hydrol. Subcomm.

611   Joe, H., 2015. Dependence modeling with copulas, Monographs on Statistics and Applied Probability.
612   CRC Press, Boca Raton, FL.

613   Kjeldsen, T.R., Jones, D.A., 2009. An exploratory analysis of error components in hydrological
614   regression modeling. Water Resour. Res. 45, W02407. https://doi.org/10.1029/2007WR006283

615   Kjeldsen, T.R., Jones, D.A., 2007. Estimation of an index flood using data transfer in the UK.
616   Hydrological Sciences Journal 52, 86–98. https://doi.org/10.1623/hysj.52.1.86

617   Kjeldsen, T.R., Jones, D.A., 2004. Sampling variance of flood quantiles from the generalised logistic
618   distribution estimated using the method of L-moments. Hydrol. Earth Syst. Sci. 8, 183–190.
619   https://doi.org/10.5194/hess-8-183-2004

620   Kroll, C.N., Stedinger, J.R., 1998. Regional hydrologic analysis: Ordinary and generalized least squares
621   revisited. Water Resour. Res. 34, 121–128. https://doi.org/10.1029/97WR02685

622   Lindskog, F., Mcneil, A., Schmock, U., 2003. Kendall's tau for elliptical distributions. Credit risk:
623   Measurement, evaluation and management 149–156.

624   Madsen, H., Mikkelsen, P.S., Rosbjerg, D., Harremoës, P., 2002. Regional estimation of rainfall intensity-
625   duration-frequency curves using generalized least squares regression of partial duration series
626   statistics. Water Resour. Res. 38, 1239. https://doi.org/10.1029/2001WR001125

627   Madsen, H., Rosbjerg, D., 1997. Generalized least squares and empirical bayes estimation in regional
628   partial duration series index-flood modeling. Water Resour. Res. 33, 771–781.
629   https://doi.org/10.1029/96WR03850

630   Meigh, J.R., Farquharson, F.A.K., Sutcliffe, J.V., 1997. A worldwide comparison of regional flood
631   estimation methods and climate. Hydrological Sciences Journal 42, 225–244.
632   https://doi.org/10.1080/02626669709492022

633   Merz, R., Blöschl, G., 2005. Flood frequency regionalisation—spatial proximity vs. catchment attributes.
634   Journal of Hydrology 302, 283–306. https://doi.org/10.1016/j.jhydrol.2004.07.018

635   Murtagh, F., Legendre, P., 2014. Ward's Hierarchical Agglomerative Clustering Method: Which
636   Algorithms Implement Ward's Criterion? J Classif 31, 274–295. https://doi.org/10.1007/s00357-
637   014-9161-z

638   Nelsen, R.B., 2006. An introduction to copulas. Springer.

639   Neves, M., Gomes, D., 2011. Geostatistics for spatial extremes. A case study of maximum annual rainfall
640   in Portugal**. Procedia Environmental Sciences 7, 246–251.
641   https://doi.org/10.1016/j.proenv.2011.07.043

642   Önöz, B., Bayazit, M., 2012. Block bootstrap for Mann–Kendall trend test of serially dependent data.
643   Hydrol. Process. 26, 3552–3560. https://doi.org/10.1002/hyp.8438

644   Ouarda, T.B.M.J., Bâ, K.M., Diaz-Delgado, C., Cârsteanu, A., Chokmani, K., Gingras, H., Quentin, E.,
645   Trujillo, E., Bobée, B., 2008. Intercomparison of regional flood frequency estimation methods at
646   ungauged sites for a Mexican case study. Journal of Hydrology 348, 40–58.
647   https://doi.org/10.1016/j.jhydrol.2007.09.031

648   Ouarda, T.B.M.J., Girard, C., Cavadias, G.S., Bobée, B., 2001. Regional flood frequency estimation with
649   canonical correlation analysis. Journal of Hydrology 254, 157–173.
650   https://doi.org/10.1016/S0022-1694(01)00488-7

651   Oudin, L., Kay, A., Andréassian, V., Perrin, C., 2010. Are seemingly physically similar catchments truly
652   hydrologically similar? Water Resources Research 46, n/a–n/a.
653   https://doi.org/10.1029/2009WR008887

654   R Core Team, 2017. R: A Language and Environment for Statistical Computing. R Foundation for
655   Statistical Computing, Vienna, Austria.

656   Reis, D.S., Stedinger, J.R., Martins, E.S., 2005. Bayesian generalized least squares regression with
657   application to log Pearson type 3 regional skew estimation. Water Resour. Res. 41, W10419.
658   https://doi.org/10.1029/2004WR003445

659   Renard, B., 2011. A Bayesian hierarchical approach to regional frequency analysis. Water Resour. Res.
660   47, W11513. https://doi.org/10.1029/2010WR010089

661   Ribeiro-Corréa, J., Cavadias, G.S., Clément, B., Rousselle, J., 1995. Identification of hydrological
662   neighborhoods using canonical correlation analysis. Journal of Hydrology 173, 71–89.
663   https://doi.org/10.1016/0022-1694(95)02719-6

664   Robson, A., Reed, D., 1999. Flood estimation handbook. Institute of Hydrology, Wallingford.

665   Salas, J.D., Heo, J.H., Lee, D.J., Burlando, P., 2013. Quantifying the Uncertainty of Return Period and
666   Risk in Hydrologic Design. Journal of Hydrologic Engineering 18, 518–526.
667   https://doi.org/10.1061/(ASCE)HE.1943-5584.0000613

668   Salinas, J.L., Castellarin, A., Kohnová, S., Kjeldsen, T.R., 2014a. Regional parent flood frequency
669   distributions in Europe – Part 2: Climate and scale controls. Hydrol. Earth Syst. Sci. 18, 4391–
670   4401. https://doi.org/10.5194/hess-18-4391-2014

671   Salinas, J.L., Castellarin, A., Viglione, A., Kohnová, S., Kjeldsen, T.R., 2014b. Regional parent flood
672   frequency distributions in Europe – Part 1: Is the GEV model suitable as a pan-European parent?
673   Hydrol. Earth Syst. Sci. 18, 4381–4389. https://doi.org/10.5194/hess-18-4381-2014

674   Salvadori, G., De Michele, C., Kottegoda, N., Rosso, R., 2007. Extremes in nature: an approach using
675   copulas. Springer Verlag.

676   Sandrock, G., Viraraghavan, T., Fuller, G.A., 1992. Estimation of Peak Flows for Natural Ungauged
677   Watersheds in Southern Saskatchewan. Canadian Water Resources Journal / Revue canadienne
678   des ressources hydriques 17, 21–31. https://doi.org/10.4296/cwrj1701021

679   Schabenberger, O., Gotway, C.A., 2004. Statistical methods for spatial data analysis. CRC Press.

680 Shang, H., Yan, J., Zhang, X., 2011. El Niño–Southern Oscillation influence on winter maximum daily
681   precipitation in California in a spatial model. Water Resour. Res. 47, W11507.
682   https://doi.org/10.1029/2011WR010415

683 Smith, R.L., 1985. Maximum likelihood estimation in a class of nonregular cases. Biometrika 72, 67–90.
684   https://doi.org/10.1093/biomet/72.1.67

685 Spence, C., Saso, P., Rausch, J., 2007. Quantifying the impact of hydrometric network reductions on
686   regional streamflow prediction in Northern Canada. Canadian Water Resources Journal 32, 1+.

687 Stedinger, J.R., Tasker, G.D., 1985. Regional Hydrologic Analysis: 1. Ordinary, Weighted, and
688   Generalized Least Squares Compared. Water Resour. Res. 21, 1421–1432.
689   https://doi.org/10.1029/WR021i009p01421

690 Tasker, G., Stedinger, J., 1989. An operational GLS model for hydrologic regression. Journal of
691   Hydrology 111, 361–375. https://doi.org/10.1016/0022-1694(89)90268-0

692 Tasker, G.D., 1980. Hydrologic regression with weighted least squares. Water Resources Research 16,
693   1107–1113.

694 Thomas, D., Benson, M., 1975. Generalization of streamflow characteristics from drainage-basin
695   characteristics. US Geological Survey Water-Supply Paper.

696 Vogel, R.M., Kroll, C.N., 1990. Generalized Low-Flow Frequency Relationships for Ungaged Sites in
697   Massachusetts1. JAWRA Journal of the American Water Resources Association 26, 241–253.
698   https://doi.org/10.1111/j.1752-1688.1990.tb01367.x

699 Wang, Z., Yan, J., Zhang, X., 2014. Incorporating spatial dependence in regional frequency analysis.
700   Water Resour. Res. 50, 9570–9585. https://doi.org/10.1002/2013WR014849

701 Ward, J.H., 1963. Hierarchical Grouping to Optimize an Objective Function. Journal of the American
702   Statistical Association 58, 236–244. https://doi.org/10.1080/01621459.1963.10500845

703 Westra, S., Sisson, S.A., 2011. Detection of non-stationarity in precipitation extremes using a max-stable
704   process model. Journal of Hydrology 406, 119–128. https://doi.org/10.1016/j.jhydrol.2011.06.014

705 Wood, S., 2006. Generalized additive models: an introduction with R. Chapman & Hall/CRC.

706 Wood, S.N., 2003. Thin plate regression splines. Journal of the Royal Statistical Society: Series B
707   (Statistical Methodology) 65, 95–114. https://doi.org/10.1111/1467-9868.00374

708 WSC, 2017. Water Survey of Canada [WWW Document]. URL
709   http://www.wsc.ec.gc.ca/applications/H2O/index-eng.cfm

710 Zhang, Z., Stadnyk, T.A., Burn, D.H., 2018. Identification of a broadly accepted statistical distribution
711   for at-site flood frequency analysis in Canada. Presented at the 71rst CWRA National
712   Conference, May 28 – June 1, Victoria, BC, Canada.

713 Zrinji, Z., Burn, D.H., 1994. Flood frequency analysis for ungauged sites using a region of influence
714   approach. Journal of Hydrology 153, 1–21. https://doi.org/10.1016/0022-1694(94)90184-8
715

716

Tables

Table 1: Summary statistics for runoff and catchment descriptors.

Variables	Abrv.	Min	Q1	Med	Avg	Q3	Max
Record length (yr)		20	25	36	39	48	111
mean of annual maximum discharge (m³/s)		0.2	13.4	45.6	206.9	174.1	5068.3
Basin area (km²)	area	1	146	460	2829	1992	48867
Basin compactness	comp	0.4	1.7	2.5	2.6	3.4	6.3
Basin mean slope (%)	slope	<0.1	1.2	3.6	10.5	17.1	59.0
Waterbody area (%)	wb	<0.1	0.4	1.3	3.7	4.5	38.3
Stream density (km⁻¹)	dens	<0.1	0.6	1.0	1.2	1.6	3.4
Elevation at site (m)	elev	1	181	382	474	731	1699
Mean annual precipitation (mm)	map	213	498	761	836	1052	3216

Table 2 : Performance criteria for flood quantiles using the ROI/GLS model with different distance. Calibration using predictive variance (individual) and super region.

		Individual		Super Region	
Variable	**Distance**	**NSH**	**MAD**	**NSH**	**MAD**
Q10	**PHY**	91.50	0.351	93.21	0.309
	GEO-PHY	92.05	0.337	**93.49**	**0.296**
	GEO	**92.27**	**0.322**	93.34	0.302
	PHY-GEO	91.53	0.343	93.48	0.299
	CCA	88.29	0.422	89.28	0.400
	GEO-CCA	91.93	0.346	93.31	0.308
Q100	**PHY**	88.74	0.411	90.72	0.362
	GEO-PHY	89.15	0.392	**91.05**	**0.343**
	GEO	**89.57**	**0.378**	90.80	0.351
	PHY-GEO	89.40	0.388	91.03	0.347
	CCA	84.42	0.488	85.96	0.457
	GEO-CCA	88.69	0.406	90.61	0.360

* Bold indicates best results in each column

726 **Table 3: Pooling group sizes and catchment descriptors for ROI/GLS model using GEO-PHY.**

	Super region	Size	Catchment descriptors
Q10	1	25	area + slope + wb + elev + map
	2	70	area + comp + elev + map
	3	25	area + slope + wb + elev + map
	4	60	area + slope + wb + map
	5	40	area + slope + elev + map
	6	40	area + dens + elev + map
	7	65	area + dens + slope + wb + elev + map
	8	40	area + dens + slope + wb + elev + map
Q100	1	25	area + slope + wb + elev + map
	2	25	area + comp + slope + wb
	3	25	area + slope + wb + elev
	4	60	area + slope + wb + map
	5	40	area + slope + elev + map
	6	25	area + wb + elev + map
	7	60	area + dens + wb + elev + map
	8	60	area + comp + dens + slope + wb + elev + map

727

728 **Table 4: Performance criteria for flood quantiles using the ROI/GLS model with a GEO-PHY**
729 **distance detailed by super region.**

Super region	Q10		Q100	
	NSH	MAD	NSH	MAD
1	96.40	0.188	93.13	0.236
2	89.29	0.243	83.25	0.271
3	78.72	0.240	69.72	0.290
4	83.83	0.223	75.93	0.293
5	31.00	0.618	32.23	0.625
6	75.41	0.406	65.43	0.476
7	88.44	0.353	84.85	0.380
8	93.99	0.215	90.92	0.248
Total	93.56	0.296	91.17	0.343

730

731
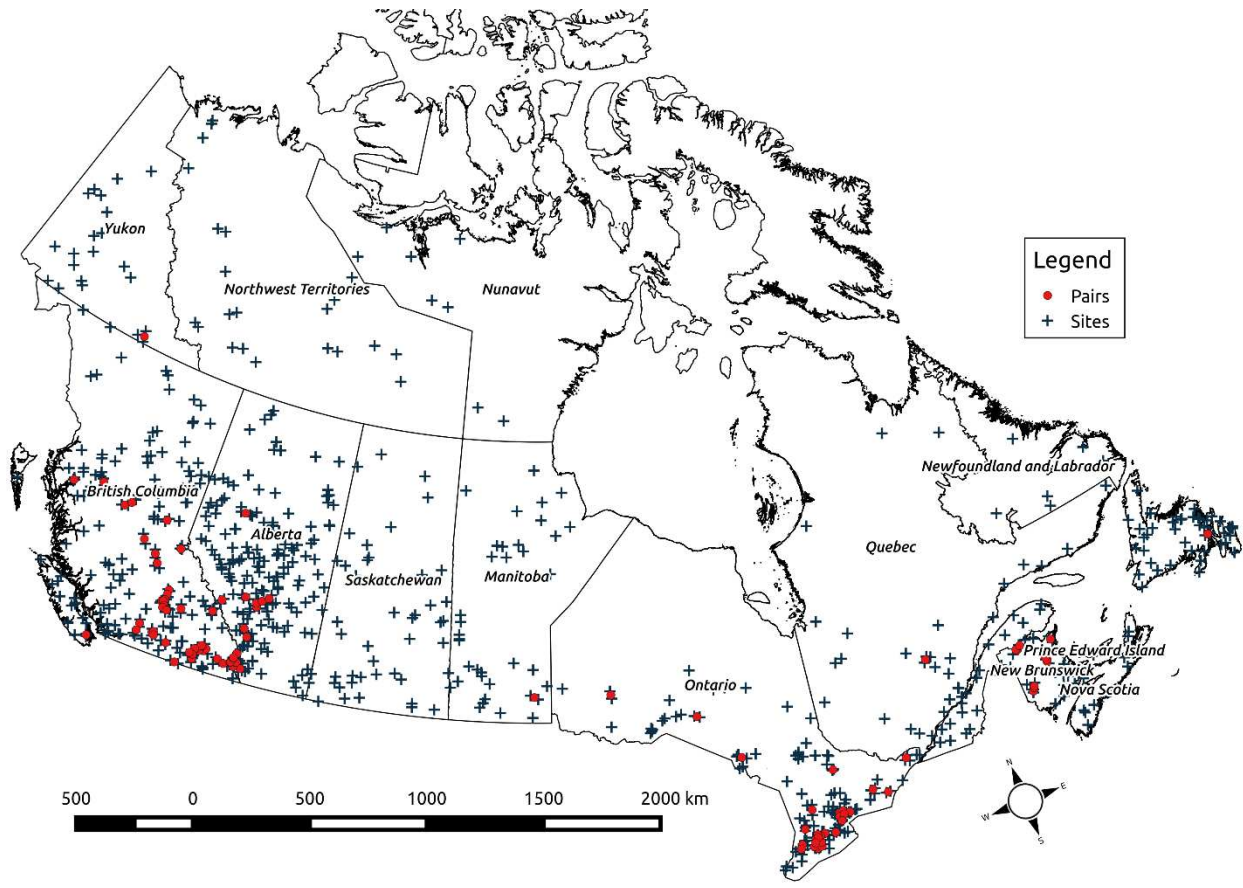
Figures
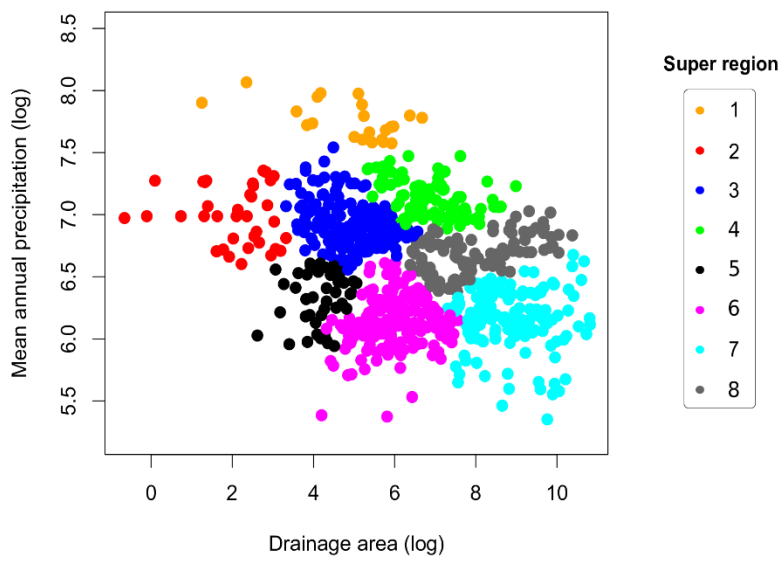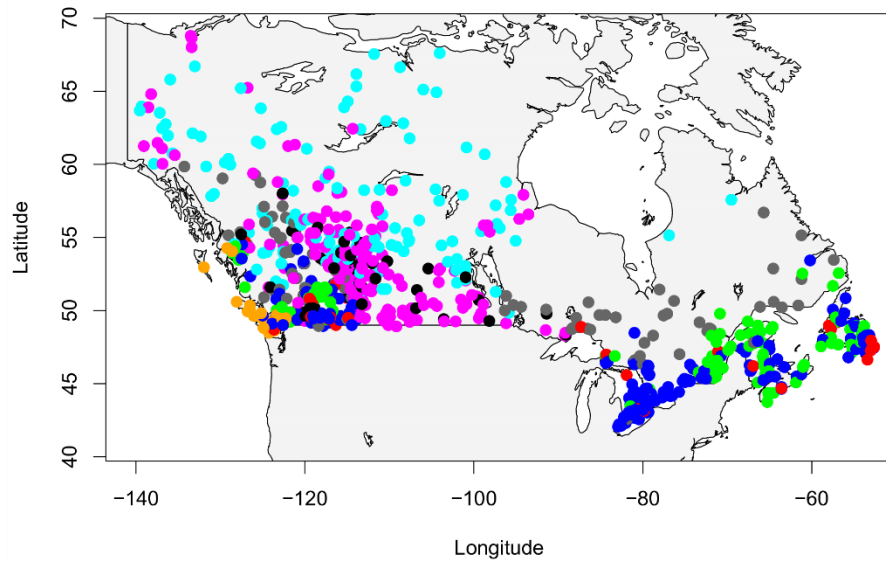
Figure 1: Locations of 771 gauged sites in Canada and average locations of 109 pairs of sites separated by less than 50 km and having 40 years of common record.
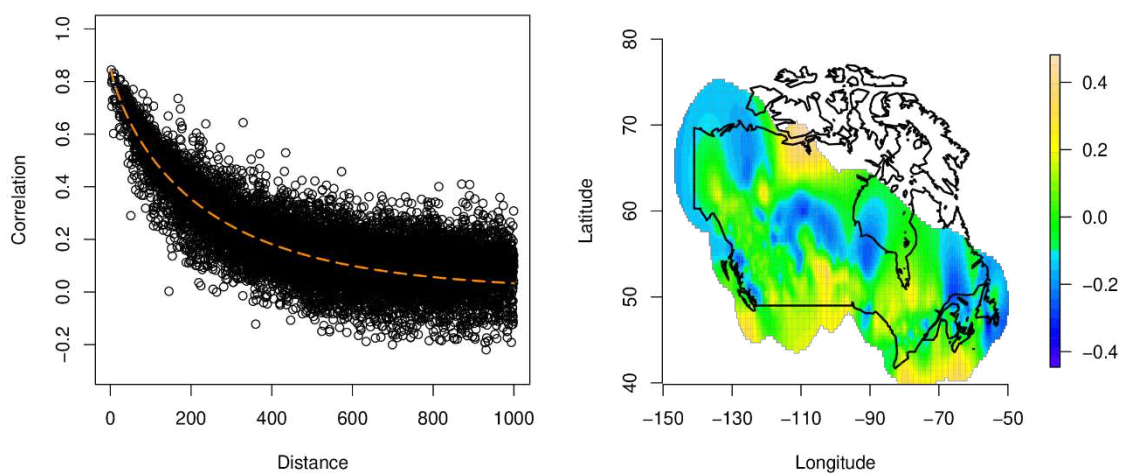
738

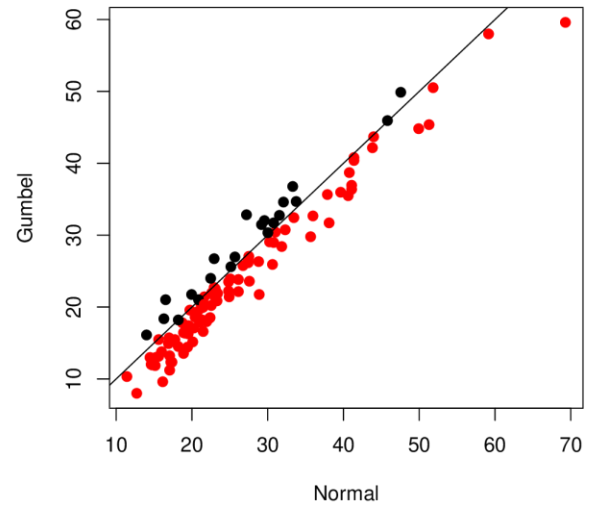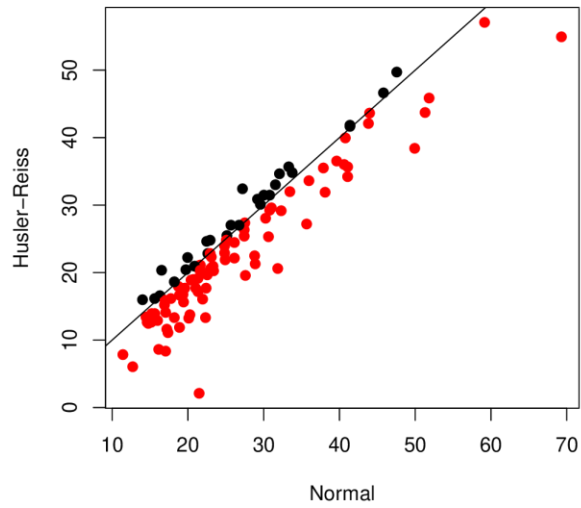**Figure 2: Super regions in geograpical (top) and descriptor space (bottom).**

740

741

742

743

Figure 3: At left, correlation coefficient estimated from the nonparametric model. The dashed line represents the fitted POW model. At right, a represention of the component f_{xy} of the nonparametric model on a grid of locations.

747

748

**Figure 4: Log-likelihood of fitted copulas for the 109 paired sites in Figure 1.**

749

750

751

752
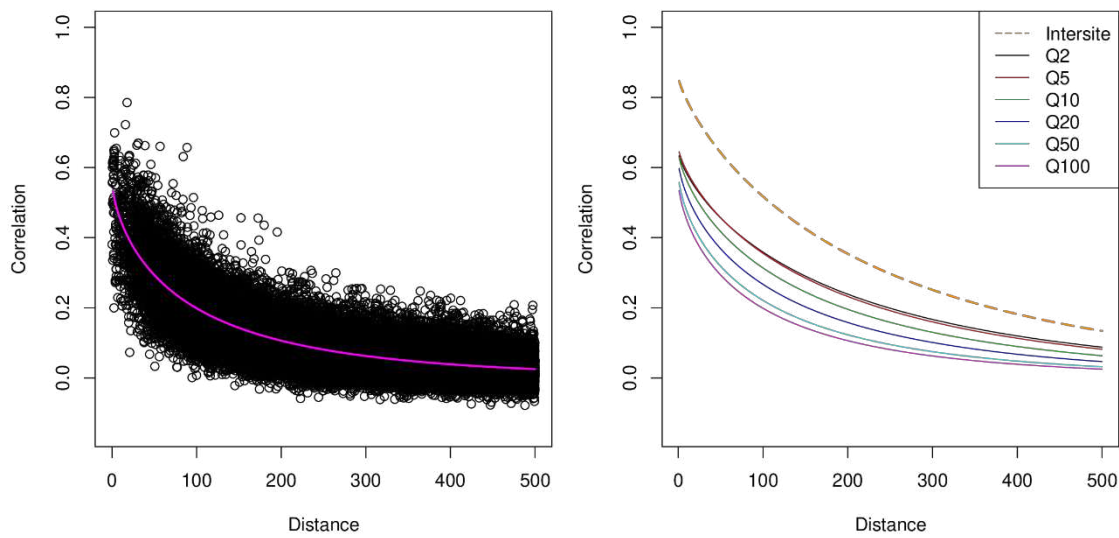
Figure 5: At left, correlation between paired Q100 (log) estimated by Monte-Carlo simulations using the nonparametric model. The solid line represents the fitted POW models. At right, the POW models are reported by return period. As a reference, the dashed line indicates the POW model for intersite correlation found in Figure 3 .
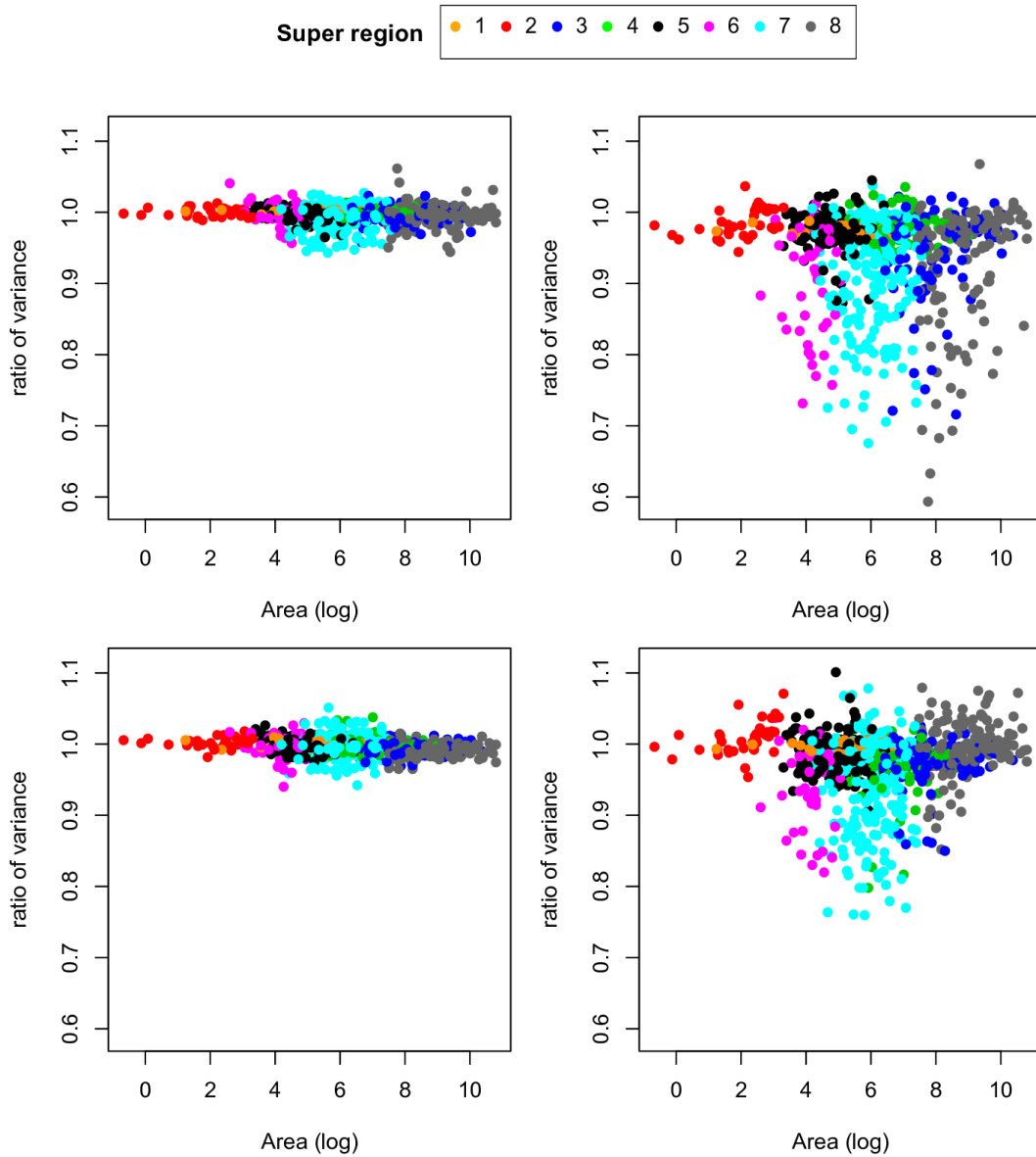
757

758

759

760
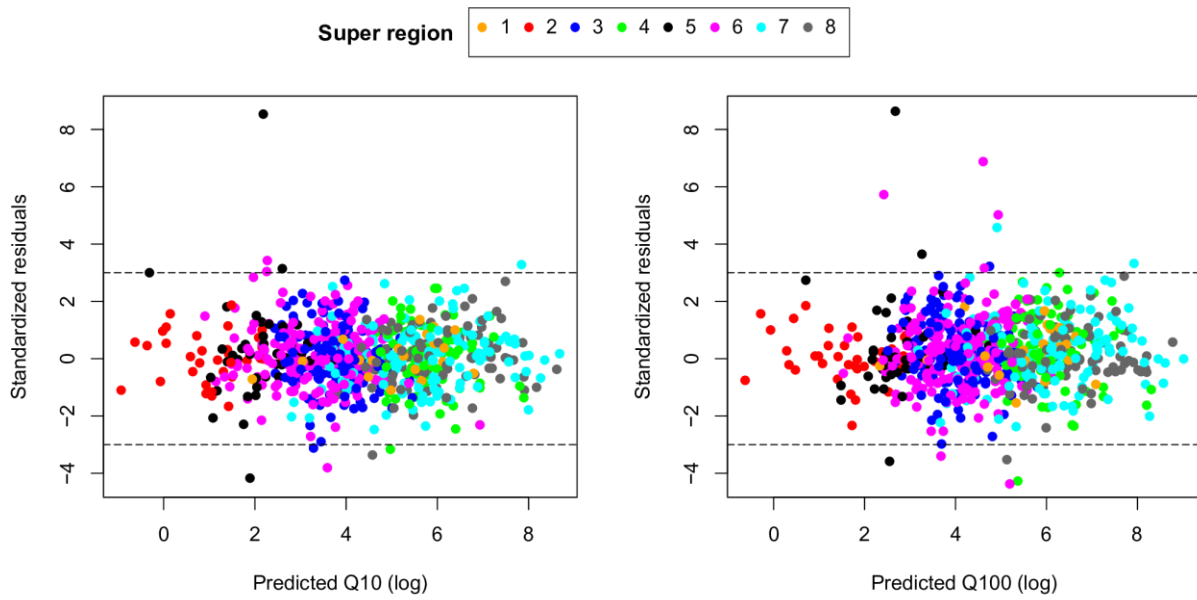
Figure 6 : Standardized predictive residuals using GEO-PHY and super regions.

Figure 7: Comparison of the ratio of predictive variance for Q10. The denominator is the predictive variance deduced from the nonparametric model, while the numerator is deduced from the POW model (left) and the assumption of independence (right). Pooling groups are formed using GEO distance (top) and GEO-PHY bottom.